Int J Ayurvedic Med,Vol 17 (2), 2026; 480-488

Ayurveda Sahiti Prabha's

International Journal of Ayurvedic Medicine

ISSN No: 0976-5921

Research Article

Impact of *Basella Alba* Leaf Mucilage on Key Variables of Clarithromycin Mucoadhesive Microspheres: Optimization Using Central Composite Design

Lalchand D Devhare[1*], Sachin Hiradeve[1], Vaibhav Uplanchiwar[1], Vinod Thakare[1]

1. Nagpur College of Pharmacy, Wanadongri, Hingna Road, Nagpur, Maharashtra, India-441110.

Received: 20-08-2025 Accepted: 17-05-2026 Published: 30-06-2026

Abstract

This study aimed to assess the mucoadhesive potential of *Basella alba* leaf mucilage (BALM) in mucoadhesive microspheres containing Clarithromycin (CMN). The objective was to evaluate how mucilage concentration influences particle size and swelling index to enhance drug delivery efficiency. A total of nine formulations were developed using Carbopol 934P (C-934P) with varying levels of BALM. The study utilized a central composite design (CCD) in Design Expert software to investigate the influence of C-934P and BALM (factors) on particle size and swelling index (responses). Formulations were further analyzed for percentage yield, drug content, release profile, and mucoadhesive belongings. Scanning electron microscope (SEM) was used to examine the structures of the microspheres. Particle size ranged from 434 ± 2.04 µm to 509 ± 1.22 µm, with batch T-9 exhibiting the smallest size and batch T-1 the largest. The swelling index varied between 62.0 ± 2.36 and 72.6 ± 2.52, increasing with higher polymer concentrations. The formulations displayed high yield, controlled drug release, excellent entrapment efficiency (EE), and strong mucoadhesion. SEM confirmed the formation of spherical microspheres with smooth surfaces. The findings demonstrate that *Basella alba* leaf mucilage significantly enhances the mucoadhesive belongings of CMN microspheres, making them suitable for gastric-specific drug delivery. This approach offers a promising strategy for improving compound retention and therapeutic efficacy in the stomach environment.

Keywords: *Basella alba,* Clarithromycin, Microspheres, Mucoadhesive, Particle size, Swelling

Access this article online

Website: https://ijam.co.in

DOI: https://doi.org/10.47552/ijam.v17i2.6480

Introduction

Gastro-retentive microspheres enhance gastric drug retention, improving bioavailability and therapeutic efficacy while ensuring patient compliance. These easy-to-prepare dosage forms prolong drug discharge in the stomach, benefiting drugs with narrow absorption windows. Their simplicity, cost-effectiveness, and ability to enhance patient adherence make them a promising innovation in drug delivery systems (DDS) (1).

Clarithromycin (CMN) is a key antibiotic in treating *Helicobacter pylori (H. pylori)* infections, often used in combination therapies to enhance efficacy and reduce resistance. It is well-absorbed orally, with a bioavailability of approximately 50%. The drug has a half-life of 3-4 h, extending to 5-7 h for its active metabolite, 14-hydroxyclarithromycin. Metabolized primarily in the liver via the CYP3A4 pathway, it inhibits bacterial protein synthesis effectively (2,3). With good patient tolerance, targeted action, and extended activity due to its metabolite, CMN remains a cornerstone in managing *H. pylori*-related conditions (4).

The need for natural polymers in pharmaceutical formulations is growing due to their biocompatibility, biodegradability, and minimal side effects compared to synthetic polymers. Synthetic polymers often raise concerns regarding environmental influence, high cost, and potential toxicities. Natural polymers from plant sources offer a safer and more sustainable alternative, aligning with the increasing demand for eco-friendly DDS (5,6).

Among natural polymers, *Basella alba L.* leaf mucilage has emerged as a promising mucoadhesive agent. Its polysaccharide-rich composition provides excellent bioadhesion, enabling extended CMN retention at the target site (stomach). This property is crucial in improving the therapeutic efficacy of drugs with poor gastric retention. Furthermore, *Basella alba* mucilage is edible, non-toxic, readily available, and cost-effective, making it a viable substitute for synthetic counterparts (7).

In the development of mucoadhesive microspheres (MMs), this mucilage enhances critical parameters such as particle size (PS) control, swelling behavior, and entrapment efficiency (EE) of CMN. It also facilitates a controlled drug discharge profile, which reduces dosing frequency and enhances patient compliance. This dual role of efficacy and safety underscores its importance in

*** Corresponding Author:**
Lalchand D Devhare
Nagpur College of Pharmacy,
Wanadongri, Hingna Road,
Nagpur, Maharashtra, India-441110.
Email Id: lalchand.devhare@gmail.com

advancing pharmaceutical technologies with a focus on eco-friendly solutions. Traditional research in DDS often explores one variable at a time for simplicity. However, this approach is limited in its ability to account for the complex interrelationships between variables, often leading to unreliable outcomes. To overcome these challenges, the Design of Experiments (DOE) methodology has emerged as a powerful tool for systematic optimization. DOE allows for the concurrent study of manifold variables, identifying their connections and collective influence on responses. This approach not only enhances the reliability of results but also reduces the number of experimental trials required, saving time and resources (8).

Factorial design (FD), a fundamental aspect of DOE, is particularly useful in pharmaceutical research. In FD, input factors are assessed at high (+1) and low (-1) levels, enabling a comprehensive evaluation of their effects. For this study, MMs of CMN were developed using a factorial design to assess the influence of 'factors', such as polymer concentrations, on outcomes like PS and SI (9).

The experimental design and optimization were carried out using Design Expert Software- 13.0 (trial version) from Stat-Ease Corporation. This software facilitated the development of a robust formula by predicting the optimal levels of input variables and their interactions to achieve desired responses. By employing such advanced techniques, the study demonstrated the potential of combining natural polymers like *Basella alba* leaf mucilage with modern statistical tools to produce superior DDS. *Basella alba* leaf mucilage exemplifies the benefits of natural polymers in pharmaceutical applications. Its integration into MMs highlights its ability to enhance drug delivery efficiency while promoting patient compliance. The use of DOE methodologies further supports the development of precise and reliable formulations, paving the way for sustainable advancements in pharmaceutical sciences (10).

The study aimed to prepare and evaluate MMs of CMN by incorporating *Basella alba* leaf mucilage to explore its mucoadhesive properties. Using CCD of Design Expert software, the impression of polymer concentrations on PS and SI was assessed, optimizing the formulation to enhance drug delivery performance. The research focused on the potential of *Basella alba* mucilage as a natural polymer for improving the efficacy of MMs in DDS.

Materials and Methods

Materials

CMN was sourced from Zydus Cadila, Ahmedabad, India. Carbopol 934P and chloroform were obtained from Merck, Ahmedabad. Other reagents used were of AR grade. Double-distilled water was used as required. *Basella alba* leaves were collected from the climbing shrub found in Ahmedabad.

Methods

Extraction of mucilage

To extract mucilage from *Basella alba* leaves using water, the collected fresh leaves were rinsed to remove dirt. The leaves were crushed and mixed with distilled water in a 1:10 ratio, heat the mixture gently at around 60±5°C while stirring to help discharge the mucilage. After 30±5 minutes, the mix was clarified over a muslin cloth to distinct the solid particles from the mucilage-rich liquid. The filtered solution was concentrated by evaporating the water content under a vacuum with a rotary evaporator (11). The mixture was then purified by precipitation with acetone (three times the quantity of the mucilage), followed by centrifugation (Remi R-303) and filtration. The mucilage was kept in an oven (Bionics Scientific, India) at 40±2°C. Finally, the mucilage was stored in a cool, dry place in an airtight container (desiccator) to prevent moisture absorption and degradation. The mucilage is now ready for use in the preparation of MMs (12).

Investigational design

Stat-Ease Software was utilized to produce and evaluate quadratic response surfaces for optimizing the *Basella alba* leaf mucilage (BALM) using a central composite design (CCD) with 9 trial runs. A quadratic model was developed to assess the influence of key, border, and quadratic factors of independent variables (IVs) on the dependent variables (DVs). The general equation for the model is:

$$Y = B_0 + B_1 X_1 + B_2 X_2 + B_{12} X_1X_2 + B_1X_1^2 + B_2X_2^2$$

In this equation, Y represents the DVs (responses), X_1 and X_2 are the IVs, and B_0, B_1, and B_2 are the regression coefficients. For BALM, the DVs were PS (Y_1) and SI (Y_2). The design consisted of 9 runs, which were carefully planned to examine the effect of the IVs and their respective levels on the responses (13). This approach allows for a comprehensive understanding of how the key factors, such as polymer concentration and processing conditions, affect the formulation's properties, enabling optimal conditions for developing BALM for use in DDS (Table 1).

Table 1: Arrangement of CMN mucoadhesive microspheres

IVs	Levels		
	Low	Medium	High
X_1= *Basella alba* leaf mucilage (mg)	50	85	120
X_2= Carbopol 934P (mg)	15	20	25
Transformed values	-1	0	1
Responses	**Goals**		
Y_1= particle size	Optimum		
Y_2= swelling index	Maximize		

Preparation of microspheres

C-934P, CMN, EC, and BALM were dissolved in a blend of dichloromethane and methanol. The resulting solution was continuously agitated in liquid paraffin containing Span 80, utilizing a propeller mixer set at 500 rpm. To induce crosslinking, 5 mL of glutaraldehyde was gradually introduced into the mixture over 3h of inspiring. The MMs were then isolated from the liquid paraffin through centrifugation and subsequently cleansed with petroleum ether to eliminate residual oil. To ensure complete removal of glutaraldehyde, the MMs were treated with a 5% v/v sodium bisulfite solution for 15 minutes and thoroughly rinsed with distilled water. Finally, the MMs were stored in a vacuum desiccator to preserve their structural integrity and prevent contamination. This meticulously controlled process ensured the fabrication of uniform MMs, making them suitable for advanced DDS (14).

Quality by Design (QbD), as outlined in ICH guidelines, serves as a fundamental framework for the development of pharmaceutical formulations. It promotes a structured methodology, beginning with the definition of a Quality Target Product Profile (QTPP) to guide formulation design and optimization. The QTPP serves as a strategic blueprint, ensuring that the final product meets predefined quality standards by integrating key product attributes into its design. This proactive methodology allows for a thorough understanding of product properties, minimizing variability and

ensuring consistency. In the development of MMs, QTPP plays a pivotal role by defining essential quality parameters, such as PS, SI, EE of CMN, and controlled drug discharge. Drawing on insights from previous research and comprehensive literature reviews, QbD principles guide the identification of Critical Quality Attributes (CQAs). These CQAs serve as measurable indicators of performance, ensuring the MMs achieve their intended therapeutic outcomes. By employing QbD and meticulously examining the QTPP and CQAs, the formulation process becomes more robust and predictable, fostering innovation while maintaining compliance with regulatory requirements. This approach underscores the importance of integrating scientific knowledge with a structured design process to optimize the quality, safety, and efficacy of MMs (15).

Evaluation

Physical assets

The particle size (PS) of the fabricated MMs was assessed using an optical microscope fitted with an eyepiece micrometer, ensuring precise measurement. To examine the shape and surface morphology, SEM was utilized. The MMs were affixed directly onto SEM sample remains with double-sided adhesive carbon tape and covered with a thin layer of platinum to enhance electrical conductivity (16).

SEM imaging was shown under a hastening voltage of 15 kV, with the compartment pressure maintained at 0.8 mm Hg, enabling high-resolution visualization of the microsphere surfaces and their structural attributes.

The flow possessions of the MMs were evaluated through key parameters such as the angle of repose (°) and Hausner's ratio (HR). The angle of repose measures the flowability of the MMs by assessing the stability of the pile formed when they are poured, while HR provides insight into their packing and compressibility. Together, these metrics ensured the MMs had favorable flow properties, which are essential for ease of handling and uniformity in pharmaceutical processes. These assessments highlight the structural integrity and physical attributes of the MMs, confirming their suitability for further applications in DDS (17).

Particle Size Measurement

The PS of the MMs was determined using a stage micrometer for accuracy. Microsphere samples were carefully placed on clean glass slides, and their dimensions were measured using an eyepiece micrometer. For each batch, 100 particles were totaled and analyzed to ensure consistent and precise size determination. This method provided reliable data for appealing the MMs, offering insights into their uniformity and suitability for their intended application. By maintaining standardized procedures, the assessment ensured reproducibility and helped evaluate the quality of MMs across different formulations effectively (18).

% yield

The % yield of MMs for different trials containing the CMN and polymers was determined by calculating the final product's weight after the drying process. This was done using Equation 1, ensuring accurate measurement and consistency across all formulations. The weight yield calculation provided essential data on the efficiency of the microsphere preparation process, reflecting the effectiveness of the method used. This evaluation is crucial for optimizing formulations, ensuring minimal wastage of materials, and achieving a desirable yield, causative to the overall success and reproducibility of the manufacturing process (19).

$$\% \text{ Yield} = \frac{\text{Weight of gainined by microspheres}}{\text{Theoritical quantity}} \text{X } 100\text{--- (1)}$$

Entrapment Efficiency

The EE was evaluated by dispersing 100 mg of MMs in 0.1 M HCl and allowing them to soak overnight. The resulting suspension was then filtered and analyzed spectrophotometrically at 210 nm using an Elico Spectrophotometer. The efficiency was resolute by comparing the quantified amount of CMN in the MMs with the initial drug quantity incorporated during formulation. This method ensured an accurate estimation of CMN entrapment, which is crucial for optimizing microsphere performance in targeted DDS. This process, as outlined in Eq. 2, ensured accurate quantification and provided insights into the effectiveness of CMN incorporation within the MMs, a critical parameter for evaluating the formulation's performance (20).

$$\text{Entrapment efficacy} = \frac{\text{Practical drug yield}}{\text{Theoritical drug content}} \text{X } 100\text{---- (2)}$$

Swelling assets

The swelling index (SI) of MMs was evaluated by immersing them in 0.1M HCl for 3 h. After this period, the MMs were detached, and centrifuged, and the weight gain was governed. The SI was calculated as the alteration between the weights at the time

(X_t) and the initial weight at time t=0 (X_0), as described in Eq.3. This method provided a measure of the MMs ability to absorb liquid, which is a critical factor in assessing their mucoadhesive and CMN delivery properties (21).

$$\% \text{ SI} = \frac{\text{Xt}-\text{Xo}}{\text{Xo}} \text{X } 100\text{--- (3)}$$

Where Xt-weight of the BALM after time t; Xo- Initial weight of the BALM.

Mucoadhesion assets

The *in vitro* wash-off tactic was employed to appraise the mucoadhesive goods of MMs. Newly cut goat intestinal mucosa sections (5.5 × 1.5 cm) were secured onto glass slides of the same size using cotton thread, and the slides were mounted on a suitable support. Approximately 50 MMs were extended over each wetted tissue specimen, and the assembly was attached to the arm of a USP disintegration test apparatus. The apparatus allowed the tissue specimen to undergo a gentle up-and-down motion in a 1L vessel containing 0.1 M HCl at 37°C (22).

The test was shown by recording the number of MMs still adhering to the tissue at intervals of 30 minutes, 1 h, and then hourly for up to 6 h. This process simulated the physiological conditions of the gastrointestinal tract, providing a reliable measure of the MMs adhesion capabilities. The number of adhered MMs was tallied at each interval, helping determine the MMs retention time and adhesion strength (23).

This method effectively demonstrated the MMs mucoadhesive assets under simulated *in vivo* conditions. The results offered valuable insights into their potential for prolonged retention in mucosal tissues, enhancing drug delivery efficacy. The formula used for these calculations is provided in Eq. 4.

$$\% \text{ mucoadhesion} = \frac{\text{Number of microspheres retained (g)}}{\text{Initial quantity of microspheres}} \text{X}100\text{--- (4)}$$

In Vitro CMN Discharge

The discharge profile of MMs was evaluated by means of the USP-II dissolution device. A speed of 100±5 rpm was maintained at 37±0.5°C. The dissolution medium entailed 900 ml of 0.1 M HCl, simulating gastric conditions. At programmed time intermissions, a 5 mL sample was withdrawn, and the dissolution medium volume was replenished to maintain consistency. These samples were analyzed spectrophotometrically at a wavelength of 210 nm to find the quantity of CMN discharged from the MMs. The spectrophotometric measurements were carried out for 10 h to assess the discharge kinetics. The data collected from these analyses were used to generate a discharge profile, enabling the determination of the cumulative amount of CMN discharged over time. This approach provides an appreciated perception of the dissolution behavior of the MMs, offering essential information for evaluating their performance as controlled-discharge DDS. The discharge pattern observed helped in understanding the potential for sustained therapeutic effects and assessing the effectiveness of the formulation for clinical application (24).

Kinetic discharge details

The CMN discharge data of the MMs were analyzed using various kinetic models. These models were labored to determine the CMN release pattern and mechanism from the MMs. By fitting the discharge data to these models, the discharge physiognomies of the formulation were evaluated, helping to understand the discharge rate and identify the dominant discharge mechanism. This analysis is crucial for optimizing the design of controlled-discharge DDS and ensuring their efficacy and sustained therapeutic action (25).

Statistical optimization

Using Design-Expert software, the IVs on responses were evaluated through 2D and 3D plots. Statistical validation of the polynomial models was performed using ANOVA, which provided critical values to assess the model's significance. The ANOVA results generated a statistical model, helping to evaluate model adequacy and predictive capability. The F-value and p-value (≤ 0.05) were key indicators for determining the robustness and accuracy of the model, ensuring its suitability for predicting the outcomes and optimizing the process under study.

Results and Discussion

Fit summary

Table 2 presents the fit summary for particle size (PS) and swelling index (SI), highlighting the suitability of different regression models within Design of Experiments. For both responses, the quadratic model demonstrated the most appropriate fit, as indicated by highly significant sequential p-values (PS: 0.0031; SI: 0.0017) along with superior adjusted and predicted R^2 values.

ANOVA details

Table 3 presents the results of Analysis of Variance (ANOVA) for evaluating the effect of independent variables (IVs) on particle size (PS) and swelling index (SI) of microspheres. The model F-values for PS (712.89) and SI (1091.94), along with highly significant p-values (<0.0001), indicate that the developed models are statistically significant and capable of explaining variability in the responses.

The ANOVA results for PS and SI responses demonstrate the arithmetical import of the factors and their interactions in optimizing the microsphere formulation.

Table 2: Regression details for the responses

PS			
Source	**Sequential p-value**	**Adjusted R^2**	**Predicted R^2**
Linear	0.0001	0.9372	0.8984
2FI	0.3726	0.9363	0.8646
Quadratic	**0.0031**	**0.9978**	**0.9937**
Cubic	1.0000		
SI			
Linear	0.0001	0.9380	0.8970
2FI	0.3372	0.9393	0.8647
Quadratic	**0.0017**	**0.9985**	**0.9956**
Cubic	0.9393	0.9961	0.9117

Table 3: ANOVA data for the IVs of microspheres

PS			
Source	**Sum of Squares**	**F-value**	**p-value**
Model	6468.78	712.89	<0.0001
A-C-934P	216.00	119.02	0.0016
B-BALM	5953.50	3280.50	<0.0001
AB	49.00	27.00	0.0138
A^2	0.8889	0.4898	0.5344
B^2	249.39	137.42	0.0013
Residual	5.44		
SI			
Model	128.91	1091.94	< 0.0001
A-C-934P	4.17	176.41	0.0009
B-BALM	118.81	5032.16	< 0.0001
AB	1.10	46.69	0.0064
A^2	0.0200	0.8471	0.4253
B^2	4.80	203.51	0.0007
Residual	0.0708		

Particle Size

The statistical analysis of the PS model demonstrated a highly significant F-value of 712.89 and a p-value of <0.0001, representing a robust fit and strong predictive capability of the model. Among the individual factors, B (BALM) had the most substantial influence on PS, with a sum of squares of 3280.50, highlighting its critical role in controlling the P. Factor A (C-934P) also exhibited a significant effect on PS, with an F-value of 119.02 and a p-value of 0.0016, signifying the combined influence of both polymers on PS. However, the quadratic term A^2 did not show a momentous influence on PS (p = 0.5344), signifying that the effect of C-934P on PS is linear rather than curvilinear. In contrast, B^2 displayed a major influence, with an F-value of 137.42 and a p-value of 0.0013, highlighting the non-linear stimulus of BALM on PS. The low residual value of 5.44 further reinforces the accuracy and precision of the model, confirming its reliability for predicting PS. These findings underscore the significant roles of both BALM and C-934P in determining PS, with BALM exhibiting a dominant effect, while the non-linear behavior of BALM concentration warrants further attention in optimizing formulations (26).

Swelling Index

The statistical analysis of the SI model revealed strong significance, with an F-value of 1091.94 and a p-value of <0.0001, settling the model's reliability. Among the factors, B (BALM) played a dominant role in influencing SI, as evidenced by its high F-value of 5032.16 and a p-value of <0.0001. Factor A (C-934P) also showed significance, with an F-value of 176.41 and a p-value of 0.0009. The interaction term (AB) was found to have a notable effect on SI (p = 0.0064), demonstrating that the combined presence of both factors influences swelling behavior. However, the quadratic term A^2 did not show a significant effect (p = 0.4253), suggesting that the influence of C-934P concentration on SI is linear rather than curvilinear. In contrast, B^2 exhibited a significant effect (F-value = 203.51, p = 0.0007), highlighting the non-linear influence of BALM concentration on SI. The minimal residual value (0.0708) further corroborates the model's precision and accuracy. Both models demonstrated excellent adequacy and predictive performance, with significant assistances from the IVs and their interactions, emphasizing BALM's critical role in determining PS and SI. The low residual values support the robustness and reliability of the models. The findings highlight the polymers' synergistic effects in controlling the MMs swelling behavior (27).

Coded equations

The coded equation for PS, derived using Design-Expert software, provides a mathematical model to predict the response based on the levels of IVs. The equation is expressed as:

$$PS= +456.56-6.00A-31.50B+3.50AB+0.6667A^2+11.17B^2$$

This equation, based on a response surface methodology (RSM) approach, represents the variables as coded factors (A and B), corresponding to the IVs in the trial, providing insights into their effects on PS and highlighting their interactions. A constant value of 456.56 represents the baseline or intercept of the model, indicating the predicted PS when all factors (A and B) are set to zero, i.e., at the central point of the trial design. The linear terms (-6.00A and -31.50B) indicate that factor A has a smaller effect on PS compared to factor B. A 1-unit upsurge in factor A consequences in a 6.00-unit decrease in PS, while factor B's 1-unit increase leads to a 31.50-unit decrease in PS. Both factors have an inverse relationship with PS, meaning as their concentrations increase, the PS decreases (28). The interaction term (3.50AB) shows a synergistic effect, meaning that when both factors increase simultaneously, PS increases by 3.50 units. The quadratic terms ($0.6667A^2$ and $11.17B^2$) indicate non-linear effects, with factor B having a more pronounced curvature effect than factor A. As factor B increases, the PS increases at a faster rate, suggesting it has a more dominant role in controlling PS.

$$SI=+65.17-0.8333A-4.45B+0.5250AB+0.1000A^2+1.55B^2$$

The intercept value 65.17 represents the predicted PS when all coded factors (A and B) are at their central or zero levels, serving as a comparison baseline. Among the linear terms, A (-0.8333) indicates that increasing the concentration of C-934P results in a slight reduction in PS. In contrast, B (-4.45) has a much larger negative coefficient, showing that increasing the concentration of BALM significantly reduces PS. This highlights the greater influence of BALM compared to C-934P in determining the PS.

The interaction term, AB (0.525), suggests a synergistic effect between C-934P and BALM, where both factors at high levels moderately increase the PS. The quadratic terms reveal non-linear effects. A^2 (-0.1) suggests that higher concentrations of C-934P exhibit minimal non-linear effects, whereas B^2 (1.55) indicates a more pronounced non-linear relationship where increasing BALM concentration beyond a certain point results in an increase in PS.

This equation is invaluable for making predictions about PS and analyzing the relative influence of each factor. It underscores BALM as the most influential variable, followed by C-934P, and helps guide formulation optimization to achieve desired PS outcomes.

Figure 1: A-H. The relation among the inputs on the responses

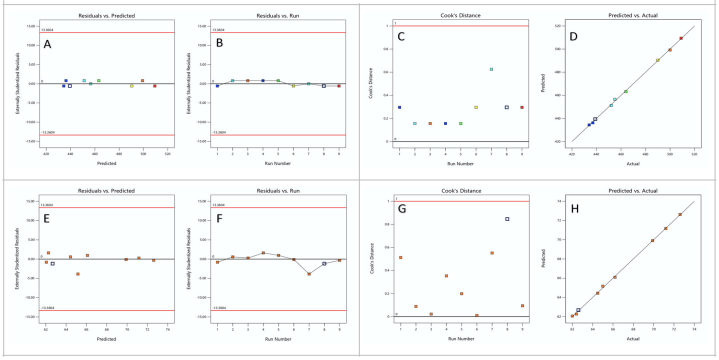

Figure 2 Presents the depiction of the PS and SI through 3D plots.

Fig.2. 2D and 3D plots for the responses

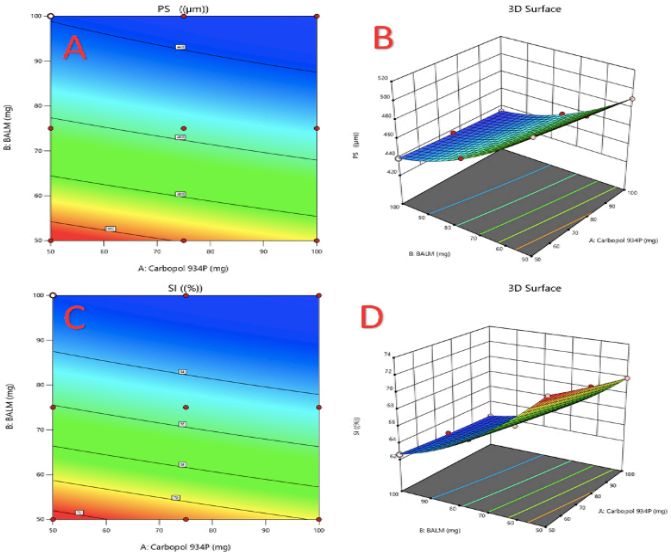

Diagnostic data

The residual plots for PS (Fig. 1A–D) revealed no important residuals, indicating that the assumption of familiarity grips. Fig. 1A shows that the residuals were consistently dispersed around zero, secondary the validity of the normality hypothesis. Additionally, the plot of residuals in contradiction with predicted values established that PS values were within acceptable limits, confirming the accuracy of the model. Fig. 1B displays an arbitrary delivery of studentized residuals, indicating that the supposition of continuous alteration was satisfied. Furthermore, residuals plotted against run numbers (Fig. 1C) showed no outliers, with all points lying within the expected range, suggesting consistent model behavior throughout the experimental runs. In Fig. 1D, the predicted and actual PS values were found to be closely aligned, further confirming the model's reliability. Similarly, the diagnostic plots for SI (Fig. 2E–H) indicated

excellent model fitting, as the residuals were aimlessly spread with no significant outliers. The predicted values for SI closely matched the observed data, indicating the accuracy of the model in predicting swelling behavior. Based on these plots, the model derived for SI using Design-Expert software provides a reliable predictive tool for analyzing the influence of IVs on swelling behavior. The equation for SI is expressed as: These plots illustrate the simultaneous influence of the factors on the DVs. Both the contour plot and the response surface plot (Fig. 2) demonstrate a consistent upsurge in response with the levels of BALM.

Optimization

The formulation conditions under study yielded a wanted PS of 446.801 µm with an SI of 63.7552%. To achieve this, the optimal amounts of C-934P and BALM were determined to be 51.1678 mg and 89.082 mg, respectively, as depicted in Fig. 3. These quantities were carefully selected to balance the desired possessions of the MMs, including size and swelling behavior, which are critical factors for DDS. The combination of C-934P and BALM played a pivotal role in optimizing the MMs. C-934P, a well-known mucoadhesive polymer, contributed to the formation of MMs with strong mucoadhesive possessions, enhancing the residence time of the CMN at the target site. On the other hand, BALM's contribution was instrumental in improving the swelling capacity of the MMs, which directly impressions the discharge profile and bioavailability of the encapsulated CMN. The results indicate that the formulation achieved the desired PS and SI within the optimal range, suggesting that the chosen concentrations of C-934P and BALM are effective in creating a stable and efficient DDS. The SI value of 63.7552% further supports the ability of the MMs to retain the CMN for extended periods, enhancing the possibility for sustained CMN release and improved therapeutic consequences.

Figure 3: Numerical illustration of Optimized results

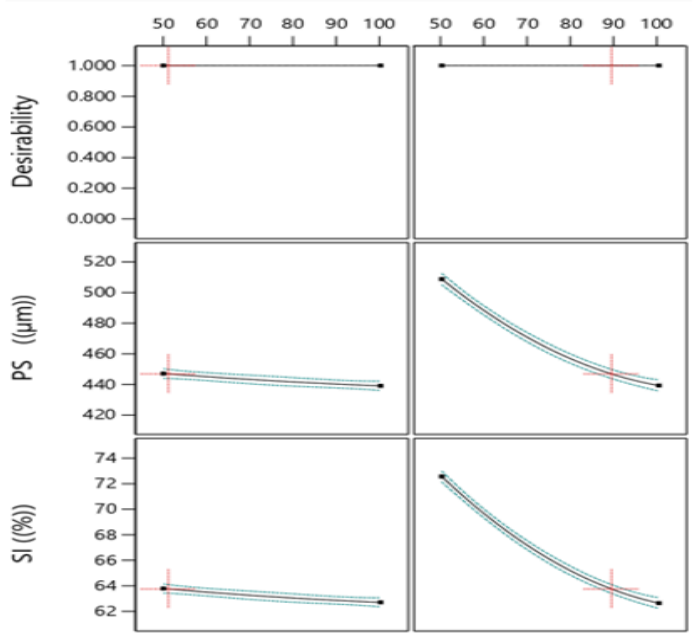

Categorization of the microspheres

SEM assets

The MMs were considered distinct, non-aggregated, and free-flowing, falling into the monolithic matrix category. They exhibited a spherical shape with a smooth surface, as shown in Fig. 4. These possessions indicate uniformity in size and structure, which are crucial for consistent drug delivery. The smooth surface and non-aggregated nature of the MMs contribute to their ideal performance in pharmaceutical applications, ensuring effective drug discharge and stability. The spherical shape also aids in maintaining uniformity during processing and enhances the MMs flowability, making them suitable for various DDS.

Figure 4: SEM picture of T-8

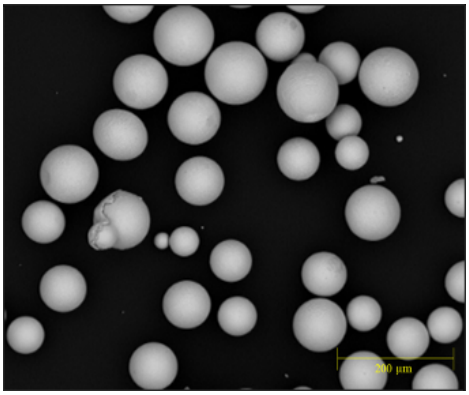

Flow assets

The MMs exhibited favorable flowability due to optimal moisture content, reduced cohesiveness, and their spherical shape. These features are essential for efficient handling and uniform supply in DDS. The angle of repose was found to be 30°, indicating good flowability, while HR ranged from 1.00 to 1.11, further confirming the excellent flow assets of the MMs (Table 4).

These results suggest that the MMs are well-suited for processing and formulation, as their flowability ensures ease of handling and consistent performance in DDS. The optimal flow physiognomies also contribute to accurate dosing, improved stability, and reliable therapeutic efficacy. Overall, the MMs demonstrated ideal assets for successful application in pharmaceutical formulations, enhancing their potential for controlled drug discharge and targeted delivery (29).

Particle size

An optical microscope was employed to analyze the size distribution and morphology of the MMs, focusing on their shape and mean diameter. The measurements were directed using a compound microscope equipped with an ocular micrometer and calibrated against a stage micrometer to ensure accuracy. At least 100 MMs were examined for each formulation to obtain reliable data on PS. The mean PS of the MMs was calculated, and the results demonstrated a consistent size distribution across batches. The diameter of the MMs ranged from 31.1±0.2 µm to 38.2±0.1 µm, as reported in Table 4. This uniformity in size suggests exactness in the manufacturing process and indicates the effectiveness of the techniques used for microsphere preparation. The uniform PS distribution is crucial for ensuring consistent drug discharge profiles, mucoadhesive assets, and the overall performance of the MMs. Optimized size distribution contributes to improved bioavailability and therapeutic efficacy by promoting uniform interaction with the mucosal surfaces. The findings underscore the importance of careful calibration and methodical examination to ensure high-quality formulations in microsphere-based DDS (30).

Yield of BALM

The % yield of the MMs was observed to range between 78.2±1.8% and 91.3±0.47%, as shown in Table 4. The yield varied across different formulations, indicating inconsistencies in the manufacturing process. A primary factor contributing to the lower yield in certain batches could be the loss of formulation components during the preparation stages. This wastage might occur due to factors such as incomplete recovery of the microsphere material, adherence to equipment surfaces, or inefficiencies in the processing steps. Despite these variations, the yield values indicate a relatively efficient production process for most formulations.

Improving manufacturing techniques, optimizing equipment design, and minimizing material losses could further enhance production yield, ensuring greater consistency. These findings highlight the importance of refining production protocols to achieve higher yields and maintain the cost-effectiveness and scalability of the microsphere formulation process.

% Drug entrapment

The EE of the MMs, as detailed in Table 4, ranged from 72.2±1.7% to 84.3±1.4%. The inclusion of BALM in the formulation significantly enhanced the EE of the MMs. This improvement is likely due to BALM's ability to interact effectively with the CMN, promoting its retention within the microsphere matrix.

However, lower EE in some formulations could be attributed to increased drug diffusion into the BALM during the preparation process. BALM's high ionization and water absorption assets may facilitate partial CMN leaching, reducing the overall efficiency. Despite this, the observed values suggest that the formulations maintained sufficient CMN entrapment for effective therapeutic action (31).

These findings underscore the influence of BALM as a functional excipient in enhancing drug encapsulation while highlighting the need for optimization to mitigate potential drug loss during processing.

Swelling assets

When immersed in 0.1 M HCl, all MMs displayed noteworthy puffiness, indicating a pronounced interaction with the acidic medium. The SI emerged as a crucial factor significantly influencing the adhesive assets and cohesiveness of the mucoadhesive polymers. A higher SI suggests enhanced hydration and swelling, which facilitate better interaction with mucosal tissue. This phenomenon occurs as MMs draw water from beneath the mucosal layer due to absorption and capillary effects, thereby strengthening their adhesion. Notably, formulations T-8 and T-9 exhibited the highest SI, attributed to their higher proportion of BALM. The superior swelling behavior of these formulations is likely a result of BALM's high ionization in acidic pH, enabling it to absorb substantial amounts of water. This distinctive contributes significantly to the adhesive potential, ensuring prolonged residence time and effective CMN delivery at the site of absorption. The results underscore the pivotal role of SI in enhancing the performance of mucoadhesive systems, particularly in acidic environments like the stomach. The ability of formulations with a higher proportion of BALM to swell extensively enhances their bioadhesive capabilities, making them suitable candidates for stomach-specific DDS. These results are summarized in Table 4, giving full visions into the swelling behavior of the formulations (32).

CMN valuation

A UV-VIS spectrophotometric method was employed to construct a calibration curve for CMN, enabling its quantification in a 0.1 M HCl solution at 210 nm. The calibration plot complied with Beer-Lambert's law over a range of 0–10 µg/mL, with triplicate measurements performed to ensure precision and repeatability. The linearity observed in the calibration curve indicates a direct proportionality between absorbance and concentration, which is critical for precise quantitative analysis. Such data is instrumental in determining the content uniformity of formulations, ensuring that the CMN concentration remains consistent across different samples or batches. This approach not only validates the reliability of the spectrometric method but also plays a vital role in quality control, enabling accurate assessment of CMN in pharmaceutical preparations. The calibration curve serves as a foundational tool for subsequent evaluations, including CMN discharge studies and formulation assessments (18).

Table 4. Flow and physical constraints of microspheres

Trial	Angle of repose (θ)	Hausner's ratio	Carr's index	Particle size (µm)	Swelling index (%)
T-1	33.05±0.41	1.024±0.02	6.37±0.28	509±1.22	72.6±2.52
T-2	29.27±0.62	1.062±0.03	7.79±0.19	500±1.64	71.2±1.98
T-3	27.39±0.94	1.028±0.01	6.80±0.18	490±1.18	69.9±1.28
T-4	28.66±0.48	1.092±0.05	8.87±0.14	464±2.52	66.2±2.17
T-5	25.47±0.37	1.021±0.04	6.48±0.62	455±3.72	65.0±1.65
T-6	26.46±0.83	1.016±0.07	6.64±0.34	452±1.15	64.5±1.54
T-7	27.98±0.44	1.094±0.06	8.68±0.11	439±2.16	62.6±1.02
T-8	28.66±0.61	1.035±0.02	5.29±0.21	437±1.74	62.4±1.25
T-9	25.88±0.43	1.026±0.03	6.65±0.08	434±2.04	62.0±2.36
Values in mean ±SD; n=3					

In vitro mucoadhesion competence

The adhesion % of the entire set of MMs with goat intestinal tissue (Fig. 5) displayed a notable correlation between binding strength and the viscosity of the polymeric material. The mucoadhesive attributes were influenced by both fluid resistance and molecular mass. In the in-vitro retention assessment, MMs containing a higher fraction of C-934P, reinforced by BALM, exhibited markedly enhanced mucoadhesive potential compared to C-934P alone. The MMs showcased exceptional bioadhesive performance, which is essential for prolonged retention at the absorption site and enhanced oral availability, as validated by the wash-off study findings (33).

Figure 5: Images indicating *ex vivo* mucoadhesion of microspheres

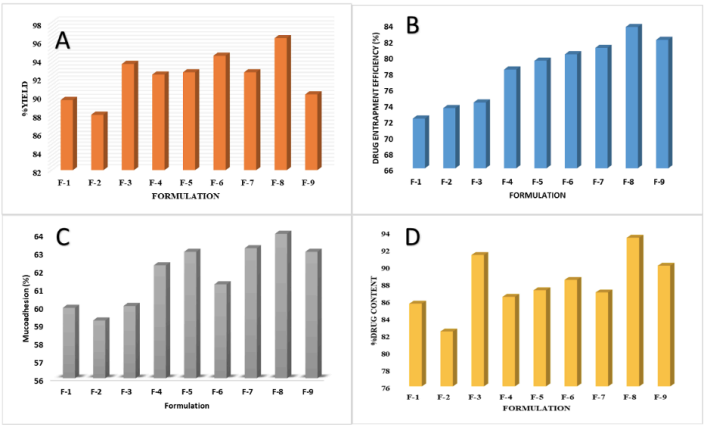

In vitro drug discharge

To evaluate the *in vitro* discharge of CMN, the MMs were tested in 0.1 M HCl for 10 h. The MMs consistently discharged CMN throughout the experiment. Figure 6 exemplifies the CMN release pattern of the MMs *in vitro*, with each formulation demonstrating a discharge period exceeding 10 h. The combination of BALM and C-934P proved effective in forming MMs. Among all formulations, T-3, T-6, and T-9 displayed the most controlled CMN discharge profile after 10 h, attributed to the higher proportion of C-934P. Upon exposure to aqueous environments, C-934P transforms into a dense gel, which plays a critical role in regulating the discharge of highly water-soluble drugs. Efficient and fast CMN discharge from hydrophilic matrices was likely driven by the swift dissolution of water-soluble drugs from the core, facilitating pore formation for solvent penetration through the spheres (34).

Figure 6: *In vitro* discharge from microspheres

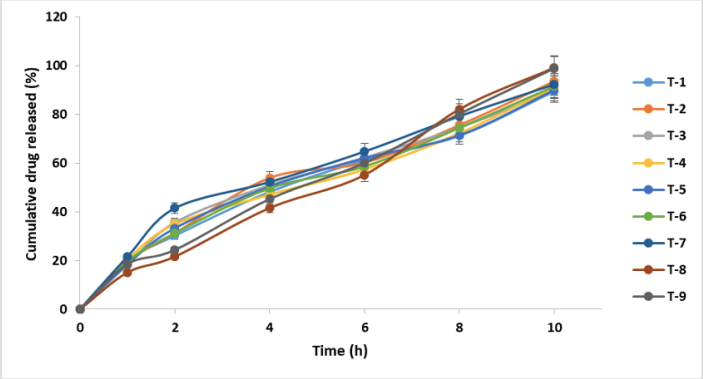

Conclusion

The study demonstrates that clarithromycin (CMN) formulated as mucoadhesive microspheres using *Basella alba* leaf mucilage (BALM) and Carbopol 934P (C-934P) effectively fulfills the criteria for an optimal mucoadhesive drug delivery system. The microspheres, considered by their smooth and spherical morphology, exhibited enhanced gastric retention and prolonged mucoadhesion. These assets are crucial for improving drug bioavailability and achieving targeted stomach-specific delivery. Overall, the formulation of CMN mucoadhesive microspheres with BALM and C-934P shows great promise in enhancing gastric residence and therapeutic efficacy.

References

1. Babu GN, Muthukarupan M, Ahad HA. Neem fruit mucilage impact on acyclovir release at different intervals: A central composite design screening. Int J Pharm Res Allied Sci. 2021;10:131–41. https : // www . ijpras . com . Accessed on 03 June 2025 at 12:15 IST.
2. Goodman LS, Brunton LL, Hilal-Dandan R, Knollmann BC. Goodman & Gilman's the pharmacological basis of therapeutics. 13th ed. New York: McGraw-Hill; 2018. https://accessmedicine.mhmedical.com/book.aspx?bookid=2189. Accessed on 22 April 2026 at 14:10 IST.
3. World Health Organization. WHO model list of essential medicines (21st list). 2019. https://www.who.int/publications/i/item/WHO-MHP-HPS-EML-2019.06. Accessed on 21 April 2026 at 15:34 IST.
4. Malfertheiner P, Megraud F, O'Morain CA, Gisbert JP, Kuipers EJ, Axon AT, El-Omar EM. Management of Helicobacter pylori infection—the Maastricht V/Florence Consensus Report. Gut. 2017;66(1):6–30. https://gut.bmj.com/content/66/1/6. Accessed on 24 April 2026 at 16:12 IST.
5. Thakur VK, Thakur MK, Gupta RK. Review on natural polymers for pharmaceutical applications. Int J Polym Anal Charact. 2019;24(4):321–345. https://www.tandfonline.com/doi/full/10.1080/1023666X.2019.1584262. Accessed on 21 April 2026 at 15:21 IST.
6. Kalia S, Avérous L, Pollet E. Biodegradable polymers. J Polym Environ. 2011;19(3):467–479. https://link.springer.com/article/10.1007/s10924-011-0317-1. Accessed on 23 April 2026 at 17:41 IST.
7. Rao KM, Suneetha M, Rao KSVK. Mucoadhesive drug delivery systems using natural polymers. Int J Biol Macromol. 2014;65:389–394. https://www.sciencedirect.com/science/article/pii/S0141813014000283. Accessed on 22 April 2026 at 15:38 IST.
8. Kumar R, Patil MB, Patil SR, Paschapur MS. Evaluation of Basella alba mucilage as a tablet binder. Int J PharmTech Res. 2010;2(1):563–567. https://www.sphinxsai.com/ptvol2no1/pharmtech_vol2no1_2010.html. Accessed on 27 April 2026 at 14:25 IST.
9. Myers RH, Montgomery DC, Anderson-Cook CM. Response surface methodology: Process and product optimization using designed experiments. 4th ed. New York: Wiley; 2016. https://onlinelibrary.wiley.com/doi/book/10.1002/9781118916014. Accessed on 25 April 2026 at 14:36 IST.
10. Babu GN, Muthukaruppan M, Ahad HA. Impact of Azadirachta indica fruit mucilage on particle size and swelling index in central composite designed acyclovir mucoadhesive microspheres. Baghdad Sci J. 2023;20:0425–. https : // bsrj . uobaghdad . edu . iq . Accessed on 12 June 2025 at 12:25 IST.
11. Ampapuram R, Subramaniyan G, Rajendran RS, Padamala RR. Gastro-protective natural polymer aided triple drug therapy to eradicate Helicobacter pylori. Pak J Pharm Sci. 2024;37. https : // pjps . pk . Accessed on 18 June 2025 at 18:05 IST.
12. Hindustan AA, Babu UA, Nagesh K, Kiran DS, Madhavi KB. Fabrication of glimepiride Datura stramonium leaves mucilage and polyvinyl pyrrolidone sustained release matrix tablets: In vitro evaluation. Kathmandu Univ J Sci Eng Technol. 2012;8:63–72. https : // www . kujset . com . Accessed on 22 July 2025 at 13:41 IST.
13. Ahad HA, Sreenivasulu R, Mallapu Rani E, Reddy BV. Preparation and evaluation of famotidine high density gastro retentive microspheres with synthetic and natural polymers. J Pharm Educ Res. 2011;2. https : // jper . in . Accessed on 02 June 2025 at 14:22 IST.
14. Ahad HA, Chinthaginjala H, Priyanka MS, Raghav DR, Gowthami M, Jyothi VN. Datura stramonium leaves mucilage aided buccoadhesive films of aceclofenac using 3^2 factorial design with Design-Expert software. Indian J Pharm Educ Res. 2021;55. https : // ijper . org . Accessed on 02 July 2025 at 15:15 IST.
15. Mundarinti S, Ahad HA. Past decade attempts on gastro retentive microspheres using factorial design: A comprehensive literature. Int J Pharm Phytopharmacol Res. 2021;11:24–30. https : // ijpppr . com . Accessed on 08 June 2025 at 13:18 IST.
16. Kumar LS, Ahad HA. Quality by design based quercetin hydrate nanoemulsions for enhanced solubility by reducing particle size. Indian J Pharm Educ Res. 2023;57:965–70. https : // ijper . org . Accessed on 08 June 2025 at 16:15 IST.

17. Mundarinti SHB, Ahad HA. Impact of Pistacia lentiscus plant gum on particle size and swelling index in central composite designed amoxycillin trihydrate mucoadhesive microspheres. Indian J Pharm Educ Res. 2023;57:763–72. https : // ijper . org . Accessed on 15 july 2025 at 14:21 IST.
18. Yadiki MN, Suggala VS, Puchalapalli DSR, Ahad HA. Temperature and exposure time impact on the extraction of Opuntia ficus-indica and Opuntia dillenii cladodes on % yield as a response: Screening using Design Expert software. Glob J Med Pharm Biomed Update. 2022;17. https : // www . gjmpbu . org . Accessed on 16 July 2025 at 16:45 IST.
19. Harsha SS, Ahad HA, Haranath C, Dasari RR, Gowthami M, Varam NJ, et al. Exfoliation technique of composing and depictions of clopidogrel bisulphate afloat microspheres. J Evol Med Dent Sci. 2020;9:1156–61. https : // jemds . com . Accessed on 16 July 2025 at 13:08 IST.
20. Syiemlieh P, Srilatha K, Ahad HA, Sequeira C, Dkhar B, Mithi J. Innovative approaches to enhance gastric retention of rabeprazole using Macrocystis pyrifera extract. 2023. https : // scholar . google . com . Accessed on 17 July May 2025 at 17:51 IST.
21. Fouziya B, Hindustan AA, Dontha SC, Jagarlamudi SV, Reddy UC, Reddy PN. Fabrication and evaluation of cefpodoxime proxetil niosomes. Asian J Pharm Technol. 2022;12:109–12. https : // ajptonline . org . Accessed on 19 July 2025 at 17:52 IST.
22. Pawar A, Lohakane P, Pandhare R, Mohite P, Munde S, Singh S, et al. Chitosan fortified repaglinide gastro-retentive mucoadhesive microsphere with improved anti-diabetic attribute. Intell Pharm. 2024;2:441–9. https : // www . sciencedirect . com . Accessed on 19 June 2025 at 13:37 IST.
23. Chechare DD, Siddaiah M. Formulation and evaluation of mucoadhesive microspheres of metronidazole. J Appl Pharm Res. 2024;12:93–9. https : // japtronline . com . Accessed on 19 July 2025 at 15:18 IST.
24. Sowjanya H, Ahad H. Mastic gum aided amoxicillin trihydrate gastro retentive mucoadhesive microspheres: In vivo evaluation. Bangladesh J Sci Ind Res. 2022;57:187–94. https : // www . banglajol . info . Accessed on 22 May 2025 at 12:46 IST.
25. Alshahrani SM, Alotaibi HF, Alqarni M. Modeling and validation of drug release kinetics using hybrid method for prediction of drug efficiency and novel formulations. Front Chem. 2024;12:1395359. https : // www . frontiersin . org . Accessed on 22 July 2025 at 18:37 IST.
26. Babu GN, Muthukarupan M, Ahad HA, Sreedhar V. Fabrication and preliminary assessment of neem fruit mucilage as mucoadhesive abetting assets with Methpol-934P for acyclovir delivery from mucoadhesive microcapsules. Biomed Pharmacol J. 2022;15:2179–84. https : // biomedpharmajournal . org . Accessed on 23 July 2025 at 17:49 IST.
27. Ahad HA, Haranath C, Vikas SS, Varam NJ, Ksheerasagare T, Gorantla SPR. A review on enzyme activated drug delivery system. Res J Pharm Technol. 2021;14:516–22. https : // rjptonline . org . Accessed on 24 July 2025 at 18:22 IST.
28. Babu GN, Menaka M, Ahad HA. Neem fruit mucilage-aided mucoadhesive microspheres of acyclovir using 3^2 factorial design with Design-Expert software. 2022. https : // scholar . google . com . Accessed on 24 July 2025 at 17:15 IST.
29. Ahad HA, Kumar CS, Kumar K, CGS S. Designing and evaluation of diclofenac sodium sustained release matrix tablets using Hibiscus rosa-sinensis leaves mucilage. Int J Pharm Sci Rev Res. 2010;1:29–31. https : // globalresearchonline . net . Accessed on 03 May 2025 at 13:22 IST.
30. Shravani Y, Ahad HA, Haranath C, Gari Poojitha B, Rahamathulla S, Rupasree A. Past decade work done on cubosomes using factorial design: A fast track information for researchers. Int J Life Sci Pharma Res. 2021;11:P124–35. https : // ijlspr . com . Accessed on 20 June 2025 at 16:28 IST.
31. Kusuma K, Subhash P, Ahad HA, Poojari SJ, Abhishek J. Deciphering the puzzle: A thorough examination of microsphere optimization through factorial design methodology, unveiling novel strategies and promising directions. Naturalista Campano. 2024;28:3143–55. https : // naturalistacampano . it . Accessed on 08 July 2025 at 16:14 IST.
32. Jwalapuram R, Ahad HA, Haranath C, Thadipatri R, Varshitha C, Kumar YB. A desktop reference to the solubility enhancement of drugs with the aid of surfactants. Int J Life Sci Pharma Res. 2020;11:P11–6. https : // ijlspr . com . Accessed on 17 June 2025 at 16:37 IST.
33. Becare Dkhar KM, Ahad HA, Sahani P, Syiemlieh P. Pushing limits: Exploring torsemide's potential through in-vitro mucoadhesive buccal delivery characterization. J Adv Zool. 2023;44. https : // jazindia . com . Accessed on 10 June 2025 at 13:36 IST.
34. Roja Y, Ahad HA, Chinthaginjala H, Soumya M, Muskan S. A glance at the literature review on buccal films. 2022. https : // scholar . google . com . Accessed on 15 July 2025 at 15:24 IST.

*****